The effect of lattice spacing change on cross-bridge kinetics in chemically skinned rabbit psoas muscle fibers

I. Proportionality between the lattice spacing and the fiber width

Masataka Kawai,* John S. Wray,‡ and Yan Zhao*

*Department of Anatomy, The University of Iowa, College of Medicine, Iowa City, IA 52242, USA; and
‡Abteilung Biophysik, Max-Planck Institut für Medizinische Forschung, D-6900 Heidelberg 1, Germany

ABSTRACT Chemically skinned rabbit psoas muscle fibers/bundles were osmotically compressed with a macromolecule dextran T-500 (0–16%, g/100 ml) at 20°C, 200 mM ionic strength, and pH 7.0. The lattice spacing of psoas bundles was measured by equatorial x-ray diffraction studies during relaxation and after rigor induction, and the results were compared with the fiber width measurements by optical microscopy. The purpose of the present study is to determine whether fiber width is a reliable measure of the lattice spacing, and to determine the available spacing for myosin cross-bridges between the thick and thin filaments. We observed that both the lattice spacing and the fiber width decreased with an increase in the dextran concentration during relaxation or after rigor induction, and that the spacing and the fiber width were proportionately related. We further observed that, in the absence of dextran, the lattice spacing (and the fiber width) shrank on a relax-to-rigor transition, whereas in the presence of 16% dextran, the spacing expanded on a relax-to-rigor transition. The cross-over of these plots occurred at the 4–7% dextran concentration. During Ca activation, the fiber width shrank in the absence of dextran, and it slightly expanded in the presence of 14.4% dextran. The degree of expansion was not as large as in the relax-to-rigor transition, and the cross-over occurred at about 11% dextran concentration. We also carried out experiments with dextran T-40 and T-10 to determine the upper limit of the molecular weight that enters the lattice space. We found that the upper limit is about 20 kD.

INTRODUCTION

During the past 30 years, it has been generally assumed that there is a compensatory mechanism in cross-bridges when the actin–myosin lattice spacing is altered by various physiological changes (H. E. Huxley, 1969). Early evidence came from the length-tension diagram that showed a linear tension decline at sarcomere lengths between 2.2 and 3.5 μm in electrically stimulated frog semitendinosus muscle fibers (Ramsey and Street, 1940; Edman, 1966; Gordon et al., 1966). In the sliding filament hypothesis (A. F. Huxley and Niedergerke, 1954; H. E. Huxley and Hansen, 1954), the number of cross-bridges involved in force generation decreases linearly as the sarcomere length increases from 2.2 to 3.5 μm. Because the actin–myosin lattice spacing of intact fibers changes in an isovolumetric manner when the sarcomere length changes, it has been assumed that the force per cross-bridge remains the same even though the distance between thick and thin filaments changes significantly (H. E. Huxley, 1969). More recently, length-tension diagrams that did not follow the linear relationship have been published (Edman and Reggiani, 1987; Grazier and Pollack, 1990). At the same time, reports demonstrating a change in isometric tension as the lattice spacing of skinned fibers was compressed osmotically have been published (Godt and Maughan, 1977, 1981; Krasner and Maughan, 1984; Kawai and Schulman, 1985). These results raise the possibility that the force-generating mechanisms may be influenced by the lattice spacing change. The following series of papers deal with this problem, and we intend to identify the elementary step(s) in the cross-bridge cycle affected by the lattice spacing change.

As initially reported by Godt and Maughan (1977) and by Maughan and Godt (1979, 1981) using skinned frog semitendinosus muscle fibers, the lattice spacing can be compressed osmotically by macromolecules such as polyvinylpyrrolidone (PVP) and dextran T-500. These macromolecules increase the osmotic pressure of the bulk solution, but they are effectively excluded from the actomyosin lattice. The consequent osmotic pressure gradient causes water and other solutes to move out from the lattice space, resulting in a compression of fibers. Several years ago we reported that low compression increased isometric tension and high compression decreased the tension in rabbit psoas fibers (Kawai and Schulman, 1985). However, in these studies we depended on the fiber width measurement to assess the lattice spacing change. Because the fiber volume is occupied not only by the contractile proteins but also by other cellular organelles, it is not established that the lattice spacing and fiber width vary in proportion. In this report, we directly measure the lattice spacing by equatorial x-ray diffraction studies, and correlate the results with the fiber width measurements. From these studies we aim to determine the actual spacing available for the myosin cross-bridge interaction with the thin filaments. Preliminary accounts of the present study have been presented in the recent symposium held in Hakone, Japan (Zhao et al., 1993).

MATERIALS AND METHODS

Chemicals and solutions

The sources of chemicals used for x-ray diffraction studies were as follows: ethylene diamine N,N,N′,N′-tetra-acetic acid (Na_2H_2EDTA),

0006-3495/93/01/187/10 $2.00

ethylene glycol-bis (beta-amino-ethyl ether) N,N'-tetra-acetic acid (H_4EGTA), adenosine 5'-triphosphate (Na_2H_2ATP), imidazole, and morpholinopropane sulfonic acid (MOPS) were purchased from Sigma Chemical Co. (Taufkirchen, Germany); $CaCO_3$, MgO, $MgCl_2$, NaOH, KOH, KH_2PO_4, K_2HPO_4, NaH_2HPO_4, Na_2HPO_4, propionic acid (HProp), and glycerol from Paesel GmbH and Co (Frankfurt, Germany). The source of chemicals used for fiber width studies were as follows: H_4EDTA, H_4EGTA, Na_2H_2ATP, $Na_{1.5}H_{1.5}ADP$, creatine phosphate (Na_2CP), MOPS were purchased from Sigma Chemical Co. (St. Louis, MO); $CaCO_3$, MgO, NaOH, KOH, KH_2PO_4, K_2HPO_4, HProp, and glycerol from Fisher Scientific Co. (Itasca, IL). Creatine kinase (CK) was purchased from Boehringer Mannheim Chemicals (Indianapolis, IN). For both studies, dextran fractions T-10, T-40, and T-500 were purchased from Pharmacia Fine Chemicals (Piscataway, NJ). All chemicals were of analytical grade.

The relaxing solution contained (mM): 6 EGTA, 2 MgATP, 5 free ATP, 8 KPi, 48 KProp, 62 NaProp, and 10 MOPS. The control activating solution contained (mM): 6 CaEGTA, 5.3 MgATP, 4.7 free ATP, 15 CP, 8 KPi, 35 KProp, 28 NaProp, 10 MOPS, and 160 units/ml of CK. The rigor-1 solution contained (mM): 10 EDTA, 8 KPi, 56 NaProp, 63 KProp, and 10 MOPS. The rigor-2 solution contained (mM): 8 KPi, 76 NaProp, 103 KProp, and 10 MOPS. In all solutions used for experiments, total Na concentration was maintained at 78 mM, ionic strength was adjusted to 200 mM with Na/KProp, and pH was adjusted to 7.00 ± 0.01. EDTA, EGTA, CaEGTA, and Pi were added as neutral K salts, MgATP and CP were added as neutral Na salts, and free ATP as $Na_2K_{1.7}ATP$ (neutral salt).

All experimental solutions were prepared without dextran, and volume and pH were adjusted. Then a given amount of dextran was added to the solution; pH did not change with this addition. The dextran concentration is expressed as a percent (%), which indicates grams of dextran added to 100 ml of solution (g/dl). When 16% dextran solution was prepared with T-500, approximately a 10% increase in the volume was noticed. Since this increase in the volume is caused by the macromolecule that is effectively excluded from the actomyosin lattice space, we assume that ionic constituents surrounding the contractile proteins do not change with this volume increase (Diamond et al., 1986). The colloid osmotic pressure of dextran solutions was measured by a computerized micro-osmometer (Multi-Osmette 2430, Precision Systems, Inc., Natick, MA) in Rigor-2 solution. The unit of the osmotic pressure reading was mOsm, and this was converted to Pascal ($=N/m^2$) by 1 mOsm = 2.436 kPa. Individual concentrations of multivalent ionic species were calculated using our computer program, which assumed multiple equilibria with the following apparent association constants (log values at pH 7.00): CaEGTA, 6.28; MgEGTA, 1.61, CaATP, 3.70; MgATP, 4.00; CaCP, 1.15; and MgCP, 1.30. pCa of activating solutions was 4.82, and pMg 3.68. pMg of the relaxing solution was 4.11. All experiments were carried out at 20°C.

Muscle preparations

Rabbit psoas bundles used for x-ray diffraction studies were prepared as described (Kawai et al., 1987). Muscle preparations used for fiber width measurements, and those used for our companion paper II were prepared as follows. New Zealand white rabbits (each weighing 3.5–5 kg) were killed by an injection of sodium pentobarbital (150 mg/kg) into an ear vein, and the psoas muscles were exposed and cooled immediately by filling the peritoneal cavity with crushed ice. Skin in the back area was removed and also cooled by ice. After 30 min in ice, fiber bundles (approximately 50 mm in length and 1 mm in diameter) were tied to bamboo sticks at in situ length with silk threads, and excised from the psoas muscle. The bundles were chemically skinned in a solution that contained (mM): 5 EGTA, 2 MgATP, 5 free ATP, 132 NaProp, 6 imidazole (pH 7.0) at 0°C for 24 h. The combination of cooling the muscle preparation before dissection and the use of Na skinning solution dramatically improved the performance of muscle preparations in the subsequent experiments over the conventional skinning procedure (Eastwood et al., 1979). Presumably, this is related to the inhibition of proteolysis by lowered temperature, and suppression of the action potential by Na skinning solution. The high ATP solution (7 mM total) also helped the preparation by keeping it relaxed during the skinning procedure. If the MgATP concentration is low, the fibers develop tension in the absence of Ca^{2+} (Reuben et al., 1971; Kawai and Brandt, 1976); excess free ATP serves as a buffer against MgATP depletion. The muscle bundles were then transferred to a storage solution (5 EGTA, 2 MgATP, 5 free ATP, 132 KProp, 6000 glycerol, 6 imidazole, pH 7.0), and kept at −20°C without freezing.

Small bundles consisting of one to two fibers each and about 10 mm in length were used for the fiber width measurements. Larger bundles of 0.3–1.0 mm diameter and about 10 mm length were used for the x-ray diffraction study. The sarcomere length was measured by optical diffraction using a He–Ne laser and adjusted to 2.5 μm. Rigor was induced by rigor-2 solution starting from the relaxing solution. After several minutes, the rigor-2 solution was replaced with the rigor-1 solution that contained EDTA to ensure more complete rigor development.

X-ray diffraction study

The x-ray source was an Elliott G18 rotating-anode generator (Marconi-Elliott, Borehamwood, England) operated at 37 kV and 50 mA. The x-ray was focused and collimated by a double-mirror camera. The muscle chamber (3 ml) was made of plexiglass with two Mylar windows separated by 1 mm, and a muscle preparation was placed between the two windows. The equatorial diffraction pattern was monitored by a one-dimensional position-sensitive counter designed and built by Dr. Klaus Rohm (Rohm, 1985). The counter was placed at 725 mm from the muscle preparation. The main beam was blocked by a center stop made of lead and placed in front of the counter. The digital images of diffraction profiles were recorded in a Nord computer, accumulated for 240 to 600 sec, and smoothed by a three-point averaging procedure. Background scattering was subtracted by linear snipping using a cross-hair cursor. Diffracted line intensity (I), peak position ($\langle i \rangle$) and width (W) were calculated by Eq. 1.

$$I = \sum_i C_i, \quad M_1 = \sum_i i \cdot C_i, \quad M_2 = \sum_i i^2 \cdot C_i$$
$$\langle i \rangle = M_1/I, \quad W = \sqrt{M_2/I - \langle i \rangle^2} \qquad (1)$$

where i is an integer and indicates the channel number, which indexes the distance along the equator (abscissae in Fig. 1). C_i is the x-ray photon count at the location i after background subtraction. Summation was performed over the appropriate diffraction line. For diffraction intensity calculation, intensities of both right and left diffraction lines were added. The lattice spacing d was calculated according to Eq. 2:

$$d = \lambda x / y \qquad (2)$$

where λ = 0.154 nm (x-ray wavelength), x = 725 mm (distance between the specimen and the detector), and y is the distance along the detector between the center and the diffraction line (0.1039 mm/channel; calibrated by collagen diffraction). The center-to-center distance of thick to thin filaments is calculated based on d_{10} and d_{11} using I_{10} and I_{11} as the weighting factors:

$$d = \frac{I_{10} d_{10}/1.5 + I_{11} d_{11}/0.866}{I_{10} + I_{11}}. \qquad (3)$$

Optical microscopy

The muscle fiber preparations were mounted in a conventional muscle chamber (capacity: 0.5 ml), and viewed from underneath by a compound microscope (Leitz Diavert; Ernst Leitz Wetzlar, GmbH., Wetzlar, Germany) with Nomarsky optics at a magnification of 200. Under our experimental conditions, cross-striations, nuclei, membrane infoldings, as well as the boundary between the fiber and the solution were clearly visible. The width of the preparation was measured by an ocular micrometer at the same point along the preparation.

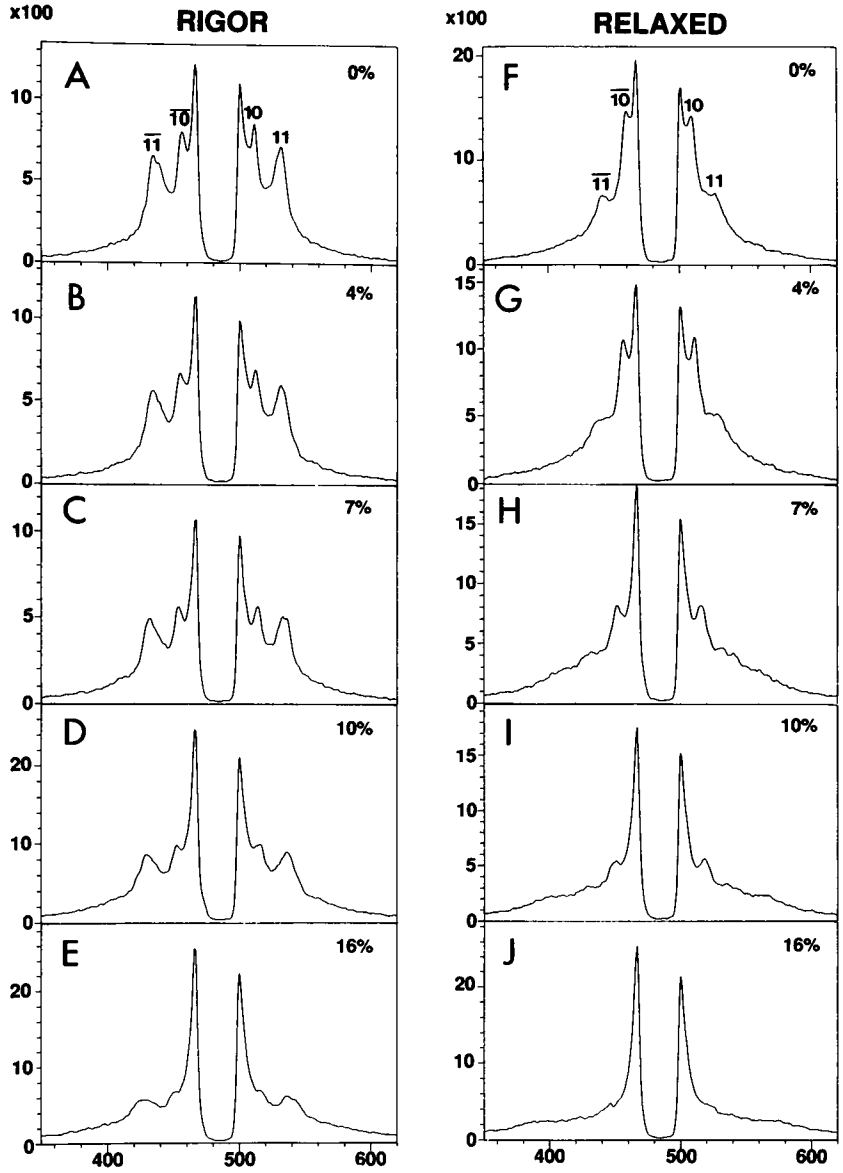

FIGURE 1 Equatorial diffraction patterns during rigor (in *A–E*) and relaxation (in *F–J*) at the dextran T-500 concentration of 0% (*A, F*), 4% (*B, G*), 7% (*C, H*), 10% (*D, I*), and 16% (*E, J*). Abscissae: channel number indicating the distance along the equator. Ordinates: photon counts. Diffraction orders 10 and 11 are identified in *A* and *F*. Exposure times are 240 s (*A, B, C*), 300 s (*G*), 450 s (*F, H, I*), and 600 s (*D, E, J*). Experiments were carried out in the order of *A* to *J*.

This was achieved by finding characteristic markers along the preparation. With activation or rigor induction, the muscle preparations did not rotate, which would have obscured the width measurement. The practical resolution of the width measurements was 2 μm. The width data were normalized to that of the relaxed preparation in the absence of dextran, and the averaging was performed on the normalized data.

RESULTS

Lattice spacing measurements

X-ray diffraction studies were carried out on relaxed and rigor muscle bundles. Small amounts of solution were continuously passed through the muscle chamber so that fresh solutions were supplied to the preparation. Rigor was induced by replacing the relaxing solution with rigor-2 solution. After a few minutes, the EDTA-containing rigor-1 solution was introduced to remove remaining Mg^{2+}. This rigor state is characterized by moderate tension and high stiffness, and is close to the "high rigor state" described by Kawai and Brandt (1976).

Fig. 1 shows typical equatorial diffraction patterns observed after rigor induction (in *A–E*) and during relaxation (in *F–J*) at dextran concentrations indicated. This particular experiment was carried out in the sequence of *A* through *J* on the same preparation. Diffraction lines 10 and 11 are evident and identified in Fig. 1 *A* and *F*. The diffraction pattern in rigor with dextran was the

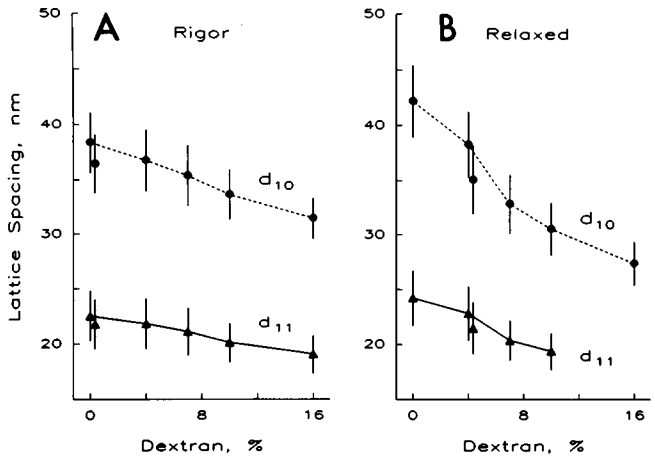

FIGURE 2 The results shown in Fig. 1 are analyzed for the peak position by Eq. 1, and the lattice spacings d_{10} and d_{11} are calculated by Eq. 2 and plotted against the dextran T-500 concentration. The widths are likewise calculated by Eqs. 1 and 2, and shown by vertical bars. The dextran concentration is increased in rigor solution in *A*, and in relaxing solution in *B*. The extra points at 0% dextran in *A* and at 4% dextran in *B* are obtained after measurements in the 16% dextran solution.

same whether the dextran was introduced before the induction of rigor or after the induction of rigor. As is well known during activation (Podolsky et al., 1976) as well as after rigor induction (H. E. Huxley, 1968), I_{11} was stronger than I_{10}, so d_{11} was primarily used for calculation of the spacing. During relaxation, I_{10} was stronger than I_{11} (H. E. Huxley, 1968), so d_{10} was primarily used for calculation of the spacing (Eq. 3).

In both rigor and relaxed conditions, it is clear that the diffraction pattern expands with an increase in the dextran concentration (Fig. 1), indicating that the lattice spacing was compressed with dextran. It is also seen that the intensity of diffraction lines decreased with an increase in the dextran concentration, implying that the lattice disorder might have increased. However, this is not due to an increase in the dispersion of the spacing, because the diffraction line width did not increase with dextran when converted to the actual distance (see below). The diffraction lines became very weak at 16% dextran (Fig. 1 *E* and *J*), and the spacing measurement was very difficult in these highly compressed states (Matsubara et al., 1985).

Based on the diffraction patterns shown in Fig. 1, the spacings d_{10} and d_{11} were calculated from Eqs. 1 and 2, and plotted in Fig. 2 against the dextran concentration. Also included are their widths in vertical bars, which were calculated by Eq. 1 and the derivative of Eq. 2. In both rigor and relaxed conditions, d_{10} and d_{11} decreased significantly with an increase in the dextran concentration. The width of the (10) or (11) reflections also decreased with an increase in the dextran concentration in both conditions; the width of (10) and (11) was approximately proportionate to d_{10} and d_{11}, respectively. When the dextran concentration was lowered from 16% to 0% in Fig. 2 *A*, and from 16% to 4% in Fig. 2 *B* (extra points in the figure), the spacing did not return to the initial condition in a few minutes. Instead, the lattice remained slightly compressed and exhibited the same spacing as at a higher dextran concentration. This observation is comparable to that of Umazume et al. (1986) on frog semitendinosus muscle fibers compressed by PVP K-30.

The center-to-center spacing of the thick and thin filaments was calculated by Eq. 3, and plotted in Fig. 3. The results show that during relaxation the lattice spacing decreased by 38% when the dextran concentration was increased from 0 to 16%. After rigor induction, the spacing decrease was 15% when the dextran concentration was increased from 0 to 16%. Furthermore, it can be seen in Fig. 3 that the plots from rigor and relaxation cross in the vicinity of 4% dextran concentration. This demonstrates that in the absence of dextran, the spacing shrinks by 8% on rigor induction, whereas in the presence of 7–16% dextran the spacing expands by 5–26% on rigor induction. The lattice spacing of intact fibers corresponds to 25.0 nm, based on d_{10} reported by Matsubara et al. (1985) on murine toe muscles. It is seen from Fig. 3 that this spacing is achieved when about 4% dextran T-500 is added both to relaxing and rigor solutions.

The intensity of the left and right diffraction lines were summed, averaged for 4–5 preparations, and plotted in Fig. 4. Fig. 4 *A* represents the intensity during relaxation,

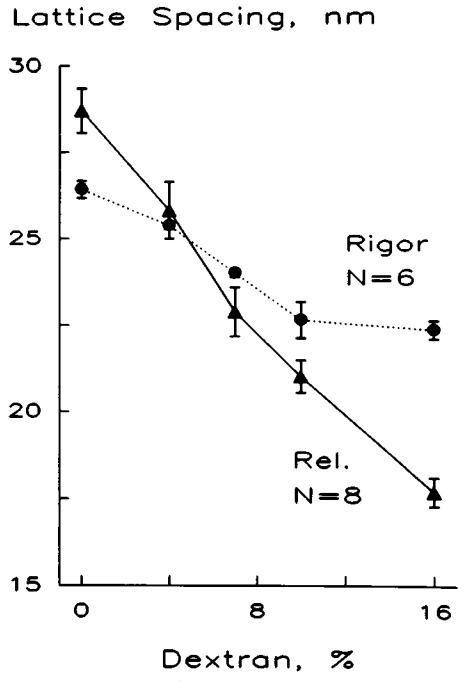

FIGURE 3 The center-to-center spacing between thin and thick filaments is plotted in nm against the dextran T-500 concentration. The data are obtained during relaxation (*triangle* and *solid line*), or after induction of rigor (*circle* and *dotted line*). The data are averaged and plotted with SEM error bars.

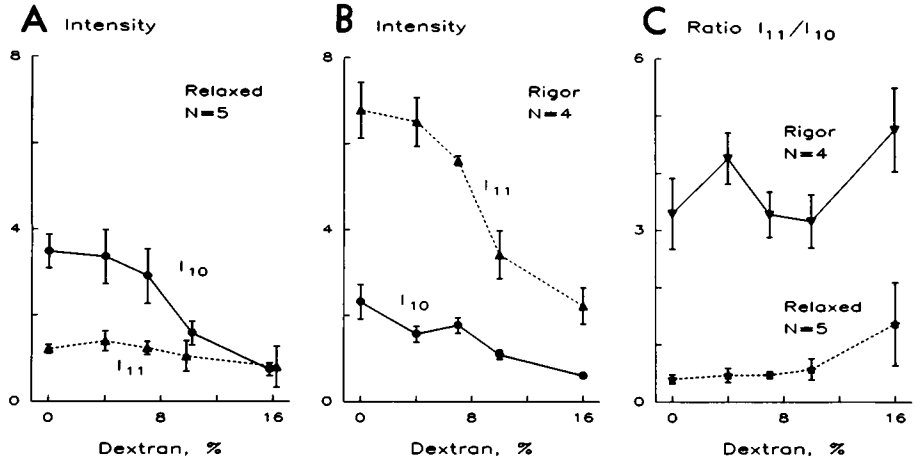

FIGURE 4 The intensity of equatorial reflections 10 and 11 is plotted against the dextran T-500 concentration. Both right and left diffraction orders are summed, and averaged without normalization. Error bars represent SEM. *A*, The data were obtained during relaxation. *B*, Data were obtained after rigor induction. Units of the ordinates in *A* and *B* are counts/s. *C*, The ratio I_{11}/I_{10} is plotted against the dextran concentration for both relaxed and rigor conditions. Ordinate is unitless.

and Fig. 4 *B* after rigor induction. Fig. 4 *C* represents the intensity ratio I_{11}/I_{10}. During relaxation, I_{10} was larger than I_{11}, and both decreased with an increase in the dextran concentration (Fig. 4 *A*). The decrease in I_{10} was greater than the decrease in I_{11}, and this resulted in a slight increase in the ratio with compression (Fig. 4 *C*). After rigor induction, I_{11} was larger than I_{10} (Fig. 4 *B*), and both decreased similarly with compression. On a transition from the relaxed to the rigor state, the loss of I_{10} was rather small (~30%) compared to the gain in I_{11} that was 3–6-fold (Fig. 4 *A* and *B*). The scatter of the data represented by SEM error bars in Fig. 4 *A* and *B* was caused primarily by the variation of the thickness of the preparations.

It is possible that the decrease in the intensity of the diffraction lines at higher dextran concentrations is caused by the increased absorption by dextran molecules. In order to test this possibility, a muscle chamber without muscle preparation was placed in the x-ray beam, the center stop removed, and the integrated intensity measured in the rigor-2 solution. In the usual optical path (approximately 1 mm), the transmitted x-ray intensity corresponded to 0.82 and 0.81 V for the solution with and without 16% dextran, respectively. When the optical path was doubled (to ~2 mm), the transmitted intensity dropped to 0.40 V both in the absence of and in the presence of dextran. These experiments demonstrate that the absorption of the x-ray beam is primarily caused by water, and not by dextran molecules.

Fiber width measurements

In the experiments shown in Fig. 5, dextran was similarly added to the experimental solution, and the fiber width was compared in the relaxed state to the rigor state in *A*, and in the relaxed state to the activated state in *B*. The rigor was induced by replacing the relaxing solution with the rigor-2 solution three to four times, and then 4 mM EDTA was introduced (rigor-1 solution) to remove the remaining MgATP. As shown in Fig. 5, the width decreased linearly with an increase in dextran concentration in all conditions. The relaxed fibers can be compressed by 40% with 16% dextran, the rigor fibers can be compressed by 20% with 16% dextran, and the active fibers can be compressed by 30% with 14.4% dextran. The plots of rigor and relaxed fibers cross in the mid-range of dextran concentration (~7%, Fig. 5 *B*). The fiber shrunk on rigor induction at low levels of compression, whereas the fiber expanded on rigor induction at

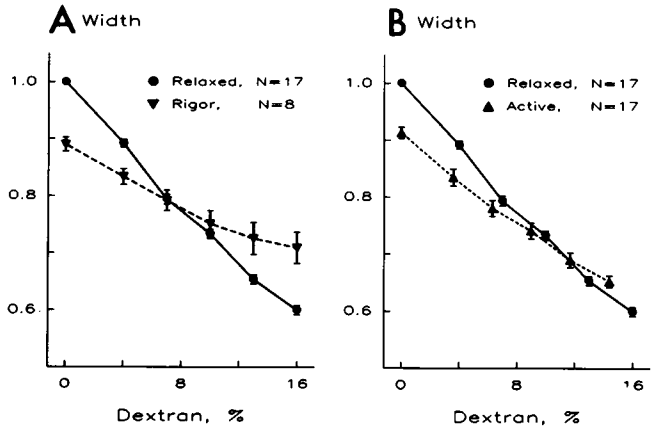

FIGURE 5 Fiber width is plotted against the dextran T-500 concentration during relaxation and after rigor induction (*A*), and during relaxation and Ca^{2+} activation (*B*). The data were normalized first to that of the relaxed preparation in the absence of dextran, then averaging was performed and plotted with SEM error bars. Dextran concentration was increased sequentially in the rigor solution without relaxing the preparation.

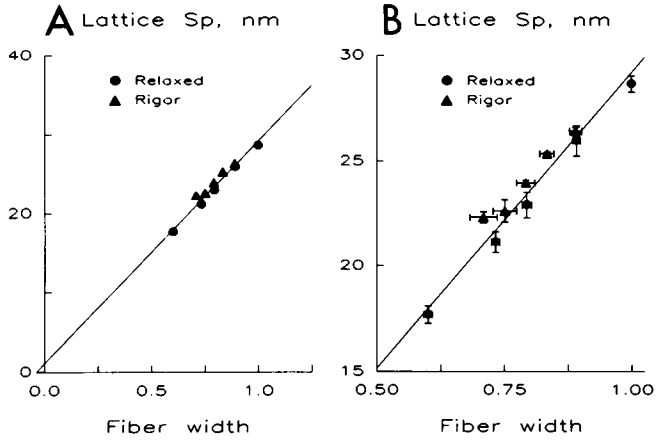

FIGURE 6 The lattice spacing (center-to-center distance between thick and thin filaments) is plotted against fiber width as these were changed by osmotic compression during relaxation and after rigor induction. The data for fiber width was obtained from Fig. 5, and the data for lattice spacing from Fig. 3. The number of experiments is 17 for relaxed width, 8 for rigor width, 8 for relaxed spacing, and 6 for rigor spacing. The *straight line* represents the linear regression line ($r = 0.986$) excluding a rigor point at 16% dextran. (*A*) Plot includes the origin; (*B*) Magnified view of the same data with SEM error bars.

high levels of compression. Similarly, the plots of active and relaxed fibers cross in the high range (10–12%, Fig. 5 *A*). The fiber shrunk on Ca-activation at the low levels of compression, whereas the fiber slightly expanded on Ca-activation at the high levels of compression. Furthermore, the width of active fibers (Fig. 5 *B*) was generally smaller than that of rigor fibers (Fig. 5 *A*) in the presence of 4–16% dextran.

The observation on the width of relaxed and rigor fibers (Fig. 5 *A*) is consistent with the lattice spacing measurement (Fig. 3). In Fig. 6, the thick-to-thin lattice spacing is plotted against the fiber width for the corresponding dextran concentrations in the relaxed and rigor preparations. This plot demonstrates a near proportional relationship between the lattice spacing and the diameter measurements in the entire range of dextran concentrations (0–16%). The regression coefficient was 0.986. A slight positive intercept in Fig. 6 *A* suggests that the fiber width may have been underestimated (about 4%).

The effect of dextran on the fiber width is generally comparable to other reports during relaxation (Godt and Maughan, 1977, 1981; Maughan and Godt, 1979; Kawai and Schulman, 1985; Matsubara et al., 1985; Arhenden et al., 1987; Tsuchiya, 1988; Roos and Brady, 1990); and after rigor induction (Podolsky et al., 1982; Millman et al., 1983; Tsuchiya, 1988).

Effect of the lower molecular weight fraction of dextran

According to the manufacturer's description, a dextran fraction is not homogeneous and the molecular weight (mol wt) is distributed. Since a lower mol wt fraction could enter the lattice space, it is suspected that this fraction may play a role in the cross-bridge kinetics (Endo et al., 1979). Thus, it is necessary to estimate the limiting mol wt of the fraction that enters the lattice space. To answer this question directly, we added smaller mol wt fractions of dextran (T-40 or T-10; Berman and Maughan, 1982) to the relaxing solution, and the fiber widths were compared. The change in the width took place in the initial 1–2 min when the dextran concentration was increased, and the width remained the same for the longest time period we observed (20 min). The results are shown in Fig. 7. As seen in this figure, T-40 and T-500 compressed the width similarly up until 10% concentration. We infer from this observation that the osmotic pressure difference inside and outside the fibers is the same whether T-40 or T-500 is used at $\leq$10% concentration.

To calculate the fraction of dextran that enters the lattice spacing, it is necessary to determine the colloid osmotic pressure of dextran solutions. For this reason we measured the osmotic pressure of T-10, T-50, and T-500 in rigor-2 solution, and the results are shown in Fig. 8. The osmotic pressure (Π) increased with concave upward as expected from the empirical Eq. 4 and the virial coefficients given by Vink (1971):

$$\Pi = A_1 c + A_2 c^2 + A_3 c^3 \qquad (4)$$

where c is the dextran concentration. The osmotic pressure data were fitted to Eq. 4, and the coefficients deduced from this fitting are included in the legend of Fig. 8. The pressure values calculated by Eq. 4 are entered in Fig. 8 as smooth curves for T-10 and T-40. As seen in

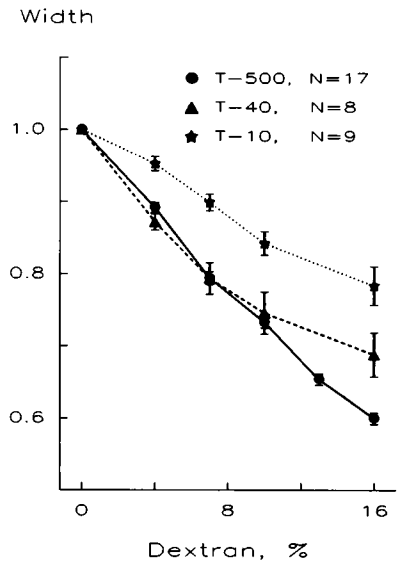

FIGURE 7 Compression of the fiber width by three dextran fractions T-10, T-40, and T-500 is compared in relaxing solution. The data for T-500 are the same as that of Fig. 5.

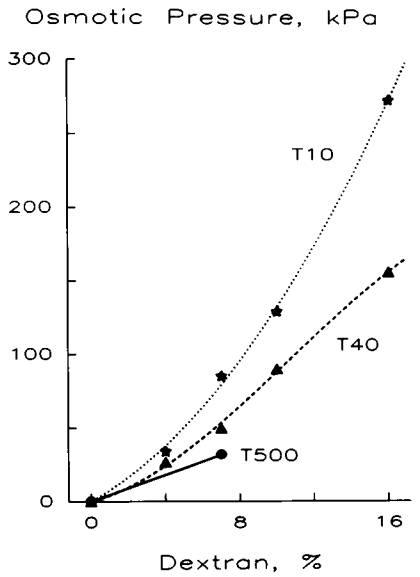

FIGURE 8 Colloid osmotic pressure of dextran solutions. The measurements were carried out in rigor-2 solution, and its osmotic pressure (390 mOsm = 950 kPa) was subtracted from the results before the data were plotted. For T-40 and T-10, the continuous curves represent the best fit to the virial expansion of the van't Hoff Eq. 4. The virial coefficients A_1, A_2, and A_3 were found to be 7.05 kPa (dl/g), 0.606 kPa $(dl/g)^2$, and 0.00115 kPa $(dl/g)^3$, respectively, for T-10; 3.26 kPa (dl/g), 0.804 kPa $(dl/g)^2$, and −0.0249 kPa $(dl/g)^3$, respectively, for T-40. Only one measurement was carried out for T-500, and this is connected to the origin by a straight line.

Fig. 8, the osmotic pressure was larger with a smaller dextran fraction, because the number of dextran molecules is larger for the same dextran concentration expressed in % (=g/dl). The osmotic pressure at 7% dextran concentration was 32 kPa (T-500), 49 kPa (T-40), and 85 kPa (T-10).

In the case of T-40, it must be concluded that the fraction corresponding to 17 kPa (=49 − 32) entered the fibers, because the osmotic pressure difference between outside and inside of fibers is the same 32 kPa in both T-40 and T-500 at 7% concentration (Fig. 7). If we solve Eq. 4 for c (or use the continuous curve labeled T40 in Fig. 8 for the same purpose), the concentration of T-40 that corresponds to Π = 32 kPa is 4.9%, hence 2.1% (=7.0 − 4.9) T-40 enters the fibers. This fraction constitutes 30% (=2.1/7.0) of T-40. The corresponding upper limit that enters the fibers is 26 kD, according to the manufacturer's mol wt distribution chart on T-40. In other words, a fraction of T-40 whose mol wt is smaller than 26 kD entered the fibers.

Compression of the fibers by dextran T-10 was half of T-500 at 7% concentration (Fig. 7). Thus, the osmotic pressure difference inside and outside the fibers is 16 kPa (=32 × 0.5) in 7% T-10, which corresponds to 2.1% T-10 in Eq. 4 or in Fig. 8. This means the fraction corresponding 4.9% (=7.0 − 2.1) T-10 entered the fibers, which amounts to 70% (=4.9/7.0) of T-10. The corresponding upper limit of mol wt is 10 kD, according to the manufacturer's mol wt distribution chart on T-10.

The shrinkage by T-10 on rabbit psoas fibers is contrary to the results of Berman and Maughan (1982) on frog semitendinosus fibers. They reported that T-10 at 18% concentration did not shrink the fiber width. It is possible that rabbit psoas and frog semitendinosus muscles respond differently to T-10. It is also possible that a skinning procedure makes a difference in the upper limit of the mol wt that will penetrate the fibers; Berman and Maughan (1982) included Triton X-100 and Briji 58 in the skinning solution, which would have made bigger pores in sarcolemma.

DISCUSSION

Proportionality between the lattice spacing and the fiber width

The most important observation in the present study is that the fiber width measured by optical microscopy is nearly proportional to the lattice spacing measured by the equatorial x-ray diffraction study (Fig. 6 *A*). The fit of the data to a regression line was excellent. The regression line passed close to the origin, and the regression coefficient was 0.986. This was true both in the relaxing condition and in the rigor condition, and their plots fell on the same regression line. A small *positive* intercept may have been caused by an optical artifact that underestimated the width of the fibers; this amounted to 3 μm in 80 μm fibers. The non-zero intercept is not due to the presence of non-myofibrillar cellular organelles, because if these contributed to the width measurement, then the intercept would have been *negative*. The good proportionality between the lattice spacing and the fiber width is convenient, because x-ray data are not always available, and they are difficult to obtain at the fast time scale such as during activation. In other words, the fiber width, when carefully measured, can index the lattice spacing in our preparations.

The good proportionality, however, may be limited to the chemically skinned rabbit psoas fibers used in the present study. The sarcolemma in this preparation becomes porous after skinning (Eastwood et al., 1979), but its mechanical constraint is present. The volume occupied by mitochondria is not as extensive as that in the slow twitch fibers or cardiac muscle preparations. If the muscle fiber is skinned mechanically as in the preparation of Natori (1954), the swelling of the fiber width is greater (Godt and Maughan, 1977), and the intermyofibrillar distance increases. Consequently, the proportionality between the fiber width and the lattice spacing does not hold as reported by Umazume et al. (1986) on mechanically skinned frog semitendinosus muscle fibers.

Compression of the lattice spacing

Another goal in this work is to document the degree of compression in the lattice spacing (or fiber width) in

chemically skinned rabbit psoas fibers/bundles when dextran T-500 is added to the bathing medium. Our results show that the lattice spacing decreased monotonically when increasing amounts of dextran T-500 were added to the bathing medium under all experimental conditions (relax, rigor, and active; Figs. 3, 5). Our results further show that in the absence of dextran the lattice spacing shrank on rigor induction, whereas in the presence of 7–16% dextran the spacing expanded on rigor induction (Fig. 3). Consequently, the plots of the lattice spacing versus dextran concentration has a crossover point in the vicinity of 4%–7% dextran concentration (Figs. 3 and 5 *A*). It is not difficult to visualize that the cross-bridge force is generated in the diagonal direction, therefore the force is divided into longitudinal and radial elements (Schoenberg, 1980). We can then recognize that the radial element helps the fiber shrink on Ca activation or on rigor induction, as happens in the absence of dextran (Figs. 3, 5).

Although the shrinkage of the width is comparable between active and rigor conditions in the absence of dextran, the expansion of the width at high dextran concentrations during Ca activation (Fig. 5 *B*) was not as large as in the rigor condition (Fig. 5 *A*), and the crossover occurred at 10–12% dextran concentration. In other words, the width of active fibers is more compressed than that of rigor fibers in the presence of dextran. This is most likely caused by the loss of the radial force element after rigor induction. With our experiments, the rigor tension (= longitudinal force element) declined close to zero by the time the width measurement was carried out. Thus it is not likely that the radial force remained at a high level. We therefore conclude that the highly compressed state during Ca^{2+} activation is caused by the continuous presence of the radial force element.

Similar observations were made on the fiber width under the relaxed and rigor conditions when mechanically skinned frog semitendinosus and adductor magnus muscle fibers were compressed by PVP K30, K40, or dextran T-70 (Maughan and Godt, 1981; Matsubara et al., 1984; Tsuchiya, 1988), and under the relaxed and activated conditions when chemically skinned rabbit soleus muscle fibers (Krasner and Maughan, 1984) and psoas fibers (Kawai and Schulman, 1985) were compressed by dextran T-500. These observations demonstrated that in the absence of compression (no dextran), the lattice shrank on Ca activation or rigor induction, whereas when the lattice was osmotically compressed the lattice expanded on Ca activation or rigor induction.

Intensity effects

It is interesting to note that the intensity of the equatorial diffraction patterns decreased with compression both during relaxation and after rigor induction (Fig. 4). The intensity decrease is larger in I_{10} than in I_{11} during relaxation (Fig. 4, *A* and *C*). This fact implies that the myosin heads are closer to the thin filament with compression, as expected during relaxation.

There could be several explanations for the decrease in intensity of the diffraction peaks: (1) an increased absorption of the x-ray beam by the dextran solution, (2) a decreased cross-section of diffraction caused by compression, (3) an increase in the lattice disorder (Brenner et al., 1984; Matsubara et al., 1985), or (4) in the compressed lattice, less density variation is associated with the diffracting planes (10) and (11). Our experiment using the chamber without the muscle rules out the possibility of an increased absorption by the dextran solution. The decrease in the diffraction cross-section may be significant; however, this cannot cause a change in the diffraction intensity. This is because the width of the x-ray beam is larger than the width of the muscle bundles, and that the same amount of materials is always placed in the x-ray beam: the amount of diffracted intensity is determined by the amount of muscle proteins in the x-ray beam. Since we did not observe any increase in the width of the diffraction lines (Fig. 2), the lattice disorder is unlikely to be the cause of the intensity decrease. With compression, the space occupied by filaments does not change, whereas the inter-filament space occupied by cytosol (solution) decreases. Therefore, reduced contrast could well explain the weakening of diffraction intensity at high dextran concentrations.

Upper limit of the molecular weight of dextran that enters the lattice space

We observed shrinkage of skinned fibers by two lower mol wt fractions of dextran T-40 and T-10 (Fig. 7). Since we can use a skinned fiber as an osmometer, and the decrease of the width corresponds to the difference of the osmotic pressure between inside (lattice space to be specific) and outside of the fibers, we can calculate the fraction of dextran that enters the fibers. For this calculation, we also need information on the total osmotic pressure of the dextran solution, which we measured (Fig. 8). The concentration dependence of the osmotic pressure for T-40 and T-500 are consistent with that calculated based on the van't Hoff equation with virial expansion and virial coefficients (A_1, A_2, A_3) given by Vink (1971). This demonstrates that the ratio $A_1:A_2:A_3$ is approximately the same between that reported by Vink (1971) and that reported in this paper (see legend of Fig. 8 for values of A_1, A_2, and A_3). However, A_1 was several times larger with our measurement, presumably owing to a variation in the batch of dextran preparations used for experiments.

Once the fraction of dextran that enters the fibers is calculated, we can then obtain the upper limit of mol wt that enters the fibers based on the manufacturer's mol wt

distribution chart. Our conclusion from experiments with T-40 is that the fraction lower than 26 kD enters the lattice space. The conclusion from experiments with T-10 is that the fraction lower than 10 kD enters the lattice space. Although these upper limit numbers do not agree precisely, their approximate agreement must be emphasized. The variation may be due to the batch of dextran fractions, and the roughness of the calculation used for these estimates. Thus, after averaging the above two results we conclude that the upper limit is about 20 kD. This information is important in evaluating the effect of T-500 on the cross-bridge kinetics, which is the subject of our companion paper II.

The authors are indebted to Professor Kenneth Holmes for continuous encouragement in the present work; to Professor Carl Gisolfi and Mr. Xiao-cai Shi for help in osmotic pressure measurements; and to Dr. Klaus Rohm and Mr. Michael P. Noel for computing help.

The present work was supported by grants from the National Institutes of Health (AR21530) and the National Science Foundation (DCB90-18096).

Received for publication 11 November 1991 and in final form 18 September 1992.

REFERENCES

Arheden, H., A. Arner, and P. Hellstrand. 1987. Force-velocity relation and rate of ATP hydrolysis in osmotically compressed skinned smooth muscle of the guinea pig. *J. Muscle Res. Cell Mot.* 8:151–160.

Berman, M. R., and D. W. Maughan. 1982. Axial elastic modulus as a function of relative fiber width in relaxed skinned skeletal muscle fibers. *Pfluegers Arch.* 393:99–103.

Brenner, B., L. C. Yu, and R. J. Podolsky. 1984. X-ray diffraction evidence for cross-bridge formation in relaxed muscle fibers at various ionic strengths. *Biophys. J.* 46:299–306.

Diamond, M. S., P. W. Brandt, and M. Kawai. 1986. Comments on "Critical dependence of calcium-activated force on width in highly compressed fibers of the frog." *Biophys. J.* 50:1215–1216.

Eastwood, A. B., D. S. Wood, K. L. Bock, and M. M. Sorenson. 1979. Chemically skinned mammalian skeletal muscle. I. The structure of skinned rabbit psoas. *Tissue and Cell,* 11:553–566.

Edman, K. A. P. 1966. The relation between sarcomere length and active tension in isolated semitendinosus fibres of the frog. *J. Physiol.* 183:407–417.

Edman, K. A. P., and C. Reggiani. 1987. The sarcomere length-tension relation determined in short segments of intact muscle fibres of frog. *J. Physiol.* 385:709–732.

Endo, M., T. Kitazawa, and Y. Kakuta. 1979. Effect of "viscosity" of the medium on mechanical properties of skinned skeletal muscle fibers. *In* Cross-Bridge Mechanisms in Muscle Contraction. H. Sugi, and G. H. Pollack, editors; University of Tokyo Press, Tokyo. 365–374.

Godt, R. E., and D. W. Maughan. 1977. Swelling of skinned muscle fibers of the frog. Experimental observations. *Biophys. J.* 19:103–116.

Godt, R. E., and D. W. Maughan. 1981. Influence of osmotic compression on calcium activation and tension in skinned muscle fibers of the rabbit. *Pfluegers Arch.* 391:334–337.

Gordon, A. M., A. F. Huxley, and F. J. Julian. 1966. The variation in isometric tension with sarcomere length in vertebrate muscle fibres. *J. Physiol.* 184:170–192.

Granzier, H. L. M., and G. H. Pollack. 1990. The descending limb of the force-sarcomere length relation revisited. *J. Physiol.* 421:595–615.

Huxley, A. F., and R. Niedergerke. 1954. Structural changes in muscle during contraction: Interference microscopy of living muscle fibres. *Nature (Lond.).* 173:971–973.

Huxley, H. E. 1968. Structural difference between resting and rigor muscle: Evidence from intensity changes in the low-angle equatorial x-ray diagram. *J. Mol. Biol.* 37:507–520.

Huxley, H. E. 1969. The mechanisms of muscular contraction. *Science (Wash. DC).* 164:1356–1366.

Huxley, H. E., and J. Hanson. 1954. Changes in the cross-striations of muscle during contraction and stretch and their structural interpretation. *Nature (Lond.).* 173:973–977.

Kawai, M. and P. W. Brandt. 1976. Two rigor states in skinned crayfish single muscle fibers. *J. Gen. Physiol.* 68:267–280.

Kawai, M., K. Güth, K. Winnikes, C. Haist, and J. C. Rüegg. 1987. The effect of inorganic phosphate on the ATP hydrolysis rate and the tension transients in chemically skinned rabbit psoas fibers. *Pfluegers Arch.* 408:1–9.

Kawai, M., and M. I. Schulman. 1985. Cross-bridge kinetics in chemically skinned rabbit psoas fibres when the actin–myosin lattice spacing is altered by dextran T-500. *J. Muscle Res. Cell Mot.* 6:313–332.

Krasner, B., and D. Maughan. 1984. The relationship between ATP hydrolysis and active force in compressed and swollen skinned muscle fibers of the rabbit. *Pfluegers Arch.* 400:160–165.

Matsubara, I., Y. E. Goldman, and R. M. Simmons. 1984. Changes in the lateral filament spacing of skinned muscle fibres when cross-bridges attach. *J. Mol. Biol.* 173:15–33.

Matsubara, I., Y. Umazume, and N. Yagi. 1985. Lateral filamentary spacing in chemically skinned murine muscles during contraction. *J. Physiol.* 360:135–84.

Maughan, D. W., and R. E. Godt. 1979. Stretch and radial compression studies on relaxed skinned muscle fibers of the frog. *Biophys. J.* 28:391–402.

Maughan, D. W., and R. E. Godt. 1981. Radial forces within muscle fibers in rigor. *J. Gen. Physiol.* 77:49–64.

Millman, B. M., K. Wakabayashi, and T. J. Racey. 1983. Lateral forces in the filament lattice of vertebrate striated muscle in the rigor state. *Biophys. J.* 41:259–267.

Natori, R. 1954. The property and contraction process of isolated myofibrils. *Jikeikai Med. J.* 1:119–126.

Podolsky, R. J., R. St. Onge, L. Yu, and R. W. Lymn. 1976. X-ray diffraction of actively shortening muscle. *Proc. Nat. Acad. Sci. (USA)* 73:813–817.

Podolsky, R. J., G. R. S. Naylor, and T. Arata. 1982. Cross-bridge properties in the rigor state. *In* Basic Biology of Muscles: A Comparative Approach. B. M. Twarog, R. J. C. Levine, and M. M. Dewey, editors. Raven Press, New York. 79–89.

Ramsey, R. W., and S. F. Street. 1940. The isometric length-tension diagram of isolated skeletal muscle fibres of frog. *J. Cell Comp. Physiol.* 15:11–34.

Reuben, J. P., P. W. Brandt, M. Berman, and H. Grundfest. 1971. Regulation of tension in the skinned crayfish muscle fiber. I. Contrac-

tion and relaxation in the absence of Ca (pCa > 9). *J. Gen. Physiol.* 57:385–407.

Rohm, K. 1985. Entwicklung und Anwendung verschiedener ortsempfindlicher Proportionalzähler fur die Röntgenstructuranalyse biologischer Objekte. Ph.D. thesis. Heidelberg University, Germany.

Roos, K. P., and A. J. Brady. 1990. Osmotic compression and stiffness changes in relaxed skinned cardiac myocytes in PVP-40 and dextran T-500. *Biophys. J.* 58:1273–1283.

Schoenberg, M. 1980. Geometrical factors influencing muscle force development. I. The effect of filament spacing upon axial forces. *Biophys. J.* 30:51–68.

Tsuchiya, T. 1988. Passive interaction between sliding filaments in the osmotically compressed skinned muscle fibers of the frog. *Biophys. J.* 53:415–423.

Umazume, Y., S. Onodera, and H. Higuchi. 1986. Width and lattice spacing in radially compressed frog skinned muscle fibres at various pH values, magnesium ion concentrations and ionic strength. *J. Muscle Res. Cell Mot.* 7:251–258.

Vink, H. 1971. Precision measurements of osmotic pressure in concentrated polymer solutions. *Eur. Polymer J.* 7:1411–1419.

Zhao, Y., M. Kawai, and J. Wray. 1993. The effect of lattice spacing change on cross-bridge kinetics in rabbit psoas fibers. *In* Mechanisms of Myofilament Sliding in Muscle Contraction. H. Sugi and G. J. Pollack, editors. Plenum Press, New York. In press.